RSC Advances

PAPER

View Article Online
View Journal | View Issue

Cite this: *RSC Adv.*, 2025, **15**, 41978

Olive leaf extract as a natural antioxidant and antimicrobial additive in biodegradable PLA film and its potential utilization in active packaging

Siwar Soltani,[a] Sawssen Hajji,[bc] Noureddine Allouche[a] and Sami Boufi[*d]

This study explores the development of a biodegradable film based on plasticized polylactic acid (PLA), incorporating olive leaf extract (OLE) to impart antimicrobial and antioxidant properties for potential use in the packaging of fruits and sensitive vegetables. Films were prepared using the casting method with triacetin as a plasticizer and three OLE concentrations (3%, 5%, and 8%). The addition of OLE induced notable changes in the colour, mechanical, and thermal properties of the films. The obtained films exhibited potent antioxidant activity and notable antibacterial effects against different bacterial strains. Migration tests, conducted by assessing the phenolic content and HPLC-DAD analysis to quantify released phenolic compounds, revealed a moderate migration rate below a 5% OLE content. Biodegradation tests demonstrated high carbon mineralization rates exceeding 50% over 60 days under burial and composting conditions. The PLA–OLE film effectively preserved high quality for 21 days at 4 °C, significantly extending the shelf life when used as active packaging for cherry tomatoes.

Received 17th June 2025
Accepted 10th October 2025

DOI: 10.1039/d5ra04293c

rsc.li/rsc-advances

1 Introduction

Plastic packaging is one of the most concerning environmental issues contributing to the growing plastic pollution disaster.[1,2] The food industry would not be without plastic—a miracle material that is highly regarded, inexpensive and easy to use. It is used by households across the country, in many cases as holders for light fittings. However, there is an environmental price for this convenience. Plastic waste has been accumulating in landfills and the oceans for years, devastating ecosystems and human health.[3]

Microplastics are minute pieces of plastic that enter the food chain and may also pose risks through chemical leaching and adverse health effects, such as hormone disruption.[4–6]

In recent years, bioplastics have been attracting increasing attention in food packaging due to increased awareness of eco-friendly solutions. These are considered promising alternatives to conventional plastic packaging, offering a more sustainable option that could reduce the dependence on petroleum-based polymers. This potential stems from their versatility and excellent biodegradability, biocompatibility and in some cases edibility.[7,8] Researchers have explored biopolymers as a greener option for food packaging; however, their poor barrier performance—particularly in terms of moisture resistance—limits their real-world application. This drawback allows water vapor to pass through, sapping freshness and leading to product spoilage and waste. While moisture-related losses remain a persistent challenge, improving moisture control is one of the most difficult obstacles to achieving truly sustainable packaging. One potential solution is to use additives in biodegradable polymer films, especially in antimicrobial and antioxidant biodegradable polymer films, to achieve multiple objectives, thus solving existing limitations, and prolonging food preservation.[9] In particular, there is a lot of interest in natural, plant-based extracts as biobased additives to develop biodegradable plastics.

Olive leaf extract (OLE), derived from the leaves of the olive tree (*Olea europaea*), is a natural bioactive substance renowned for its potent antioxidant, antimicrobial, and anti-inflammatory properties.[10–12]

Recently, various investigations have reported the incorporation of OLE into various composite film formulations. Several studies have investigated the antioxidant properties of biodegradable carrageenan films that incorporate this extract, making them suitable for food packaging applications.[13–15] Moreover, a previous study explored polylactic acid (PLA) films containing poly (ethylene glycol) as a plasticizer and olive leaf extract (OLE), prepared by a casting method,[16] while other studies utilized a coating method to prepare PLA/OLE films.[17] A blend of OLE and chitosan contributes to the development of promising antioxidant and antimicrobial food packaging

[a]*Laboratory of Organic Chemistry LR17ES08, Natural Substances Team, Faculty of Sciences of Sfax, University of Sfax, BP 802 - 3018 Sfax, Tunisia*
[b]*University of Gabes -Higher Institute of Applied Biology of Medenine, 4119 Medenine, Tunisia*
[c]*Laboratory of Enzyme Engineering and Microbiology, National School of Engineering of Sfax (ENIS), University of Sfax, 3038 Sfax, Tunisia*
[d]*University of Sfax, LMSE, Faculty of Science, BP 802 - 3018 Sfax, Tunisia. E-mail: sami.boufi@fss.rnu.tn; Fax: +216 74274437; Tel: +216 47274400*

materials.[18,19] In a study by Mohammed Sabbah *et al.* (2023), pectin films were developed with OLE, resulting in enhanced functionality and activity of the pectin-based edible film.[20] Olive leaf water/ethanol extract was also used as an antimicrobial and antioxidant ingredient in edible gelatin films for preserving cold-smoked fish.[21] Sodium alginate was also incorporated with OLE to develop bioactive films, which effectively enhance food preservation, offering a sustainable alternative to conventional packaging materials.[22]

This study aimed to design and characterize PLA-based films enriched with OLE for potential use as active packaging. To enhance the flexibility and ductility of the PLA film, the biodegradable plasticizer triacetin was incorporated. Films containing various concentrations of OLE (ranging from 0% to 8%) were prepared using the casting method, and the effects of the OLE content on the mechanical, thermal, structural, antioxidant, and antimicrobial properties of the films were thoroughly investigated. Additionally, the migration of OLE and the biodegradability of the PLA films with the additive were examined. As a practical application, the PLA–OLE films were tested as packaging for cherry tomatoes. The results provided clear evidence that the inclusion of OLE in thin PLA films effectively extended the shelf life of the tomatoes.

2 Results and discussion

2.1 Phytochemical composition of OLE

The phytochemical composition of olive leaf extract (OLE), analyzed using high-performance liquid chromatography with diode array detection (HPLC-DAD), reveals a diverse range of phenolic compounds, with their abundance varying based on the chemical composition (Table 1). Oleuropein is the predominant compound, constituting 57.22% of the extract, and is well-known for its exceptional biological properties, which include antibacterial, anti-inflammatory, and antioxidant properties.[23–25] Other noteworthy substances are verbascoside (1.74%) and hydroxytyrosol (2.02%), both of which are known to have antioxidant qualities even though they are found in lesser amounts. Although in smaller amounts, luteolin glucoside (0.85%), apigenin 7-*O*-glucoside (0.31%), and naringenin (0.65%) further add to the extract's bioactive profile. The presence of these phenolic compounds and flavonoids suggests that olive leaf extract may offer substantial antioxidant properties and health benefits. It should be noted that Table 1 reports only the major phenolic compounds of OLE, identified and quantified by HPLC-DAD using authentic reference standards. The minor constituents of the crude extract were negligible and not detectable due to the dominance of the major peaks, particularly oleuropein.

2.2 Physical properties of PLA–OLE films: mechanical, thermal, structural and colorimetry analysis

To evaluate the impact of olive leaf extract (OLE) on the mechanical properties of PLA films, tensile tests were conducted on PLA–OLE films with various OLE contents. The typical stress–strain curves are presented in Fig. 1A, from which the corresponding Young's modulus (E), strength (S), and strain at break (SB) were extracted and compiled (Fig. 1B). A decrease in E and S was observed with the addition of OLE, with reduction rates of approximately 49%/31%, 53%/36%, and 57%/44% at OLE concentrations of 3%, 5%, and 8%, respectively, compared to the neat plasticized PLA film (PLA 0%). However, no significant change was detected in the strain at break, indicating that while the PLA films became less stiff and strong with the addition of OLE, their ductility remained unaffected. Two hypotheses may explain this behavior. The first is a potential plasticizing effect induced by OLE, while the second involves changes in the crystalline structure of PLA upon OLE addition. Given the lack of significant variation in SB, the plasticizing effect is unlikely. The second hypothesis will be further examined through DSC analysis, as discussed in the following section.

The DSC thermograms of PLA films with various OLE contents are shown in Fig. 2, presenting the first heating, cooling, and second heating cycles. For comparison, the thermograms of neat PLA and plasticized PLA without OLE are also included. PLA plasticized with triacetin (PLA 0%) exhibits a lower glass-transition temperature ($T_g = 40$ °C) compared to neat PLA ($T_g = 62$ °C), confirming the effective plasticizing effect of triacetin. Whereas the melting temperature (T_m) remains relatively stable at 170 °C. Similarly, the incorporation of OLE does not significantly affect the T_g of the plasticized film, which remains at around 40 °C, nor does it alter the melting temperature, which stays stable at approximately 169 °C. However, a decrease in crystallinity was observed with increasing OLE content (Fig. 2D), with a corresponding reduction in crystallinity degree from 28% to 24% and 21% at OLE concentrations of 5% and 8%, respectively. One possible explanation for this reduction in crystallinity is the interaction between OLE's phenolic components and PLA chains, which may hinder their ability to assemble into a crystalline lattice. This decline in PLA crystallinity following OLE addition could, in turn, explain the observed reductions in the tensile modulus (E) and strength (S) of the films (Fig. 1), reported previously.

FTIR analysis of the PLA–OLE films was conducted to evaluate any potential structural changes in the PLA matrix after the addition of OLE (Fig. 3). The FTIR spectra of neat PLA and plasticized PLA (PLA 0%) were nearly identical, revealing the main functional features of PLA. Typical bands were observed at 749 cm^{-1} and 863 cm^{-1}, corresponding to the crystalline and amorphous phases of PLA, respectively.[26] The bands at 1082 cm^{-1} and 1179 cm^{-1} were attributed to the asymmetric and symmetric stretching of the complex C–O–C group, respectively.[27] Additionally, bands at 1453 cm^{-1} and 1357 cm^{-1} were assigned to the asymmetric and symmetric CH- deformation vibrations.[28] The intense band at 1744 cm^{-1} corresponds to the carbonyl group of the ester in PLA.[29] The characteristic bands of OLE appeared at 1618 cm^{-1} and 1701 cm^{-1}, corresponding to olefinic and carbonyl groups, respectively, while bands in the range of 1504–1431 cm^{-1} were attributed to aromatic rings.[30]

As shown in Fig. 3, no significant changes were observed in the FTIR spectra of the PLA–OLE films, either in band positions

Table 1 Phenolic compounds of the olive leaf extract (OLE) identified by HPLC-DAD

No.	Compound	Structure	Relative abundance (%)
1	Hydroxytyrosol	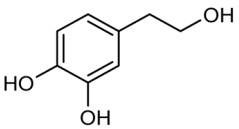	2.02
2	Verbascoside	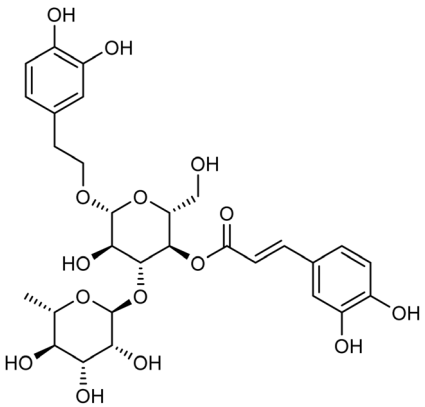	1.74
3	Luteolin glucoside	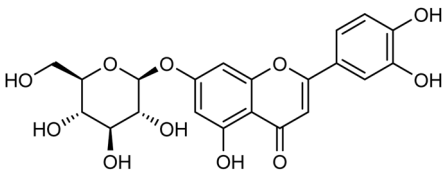	0.85
4	*P*-Coumaric acid	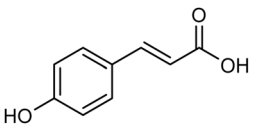	0.10
5	Apigenin 7-*O*-glucoside	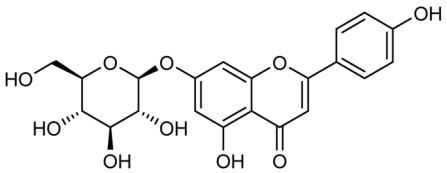	0.31
6	Oleuropein	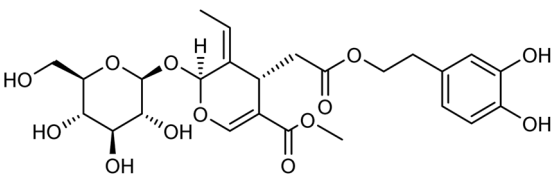	57.22
7	Naringenin	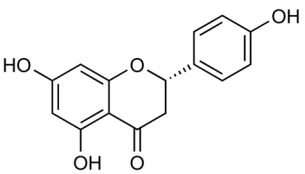	0.65

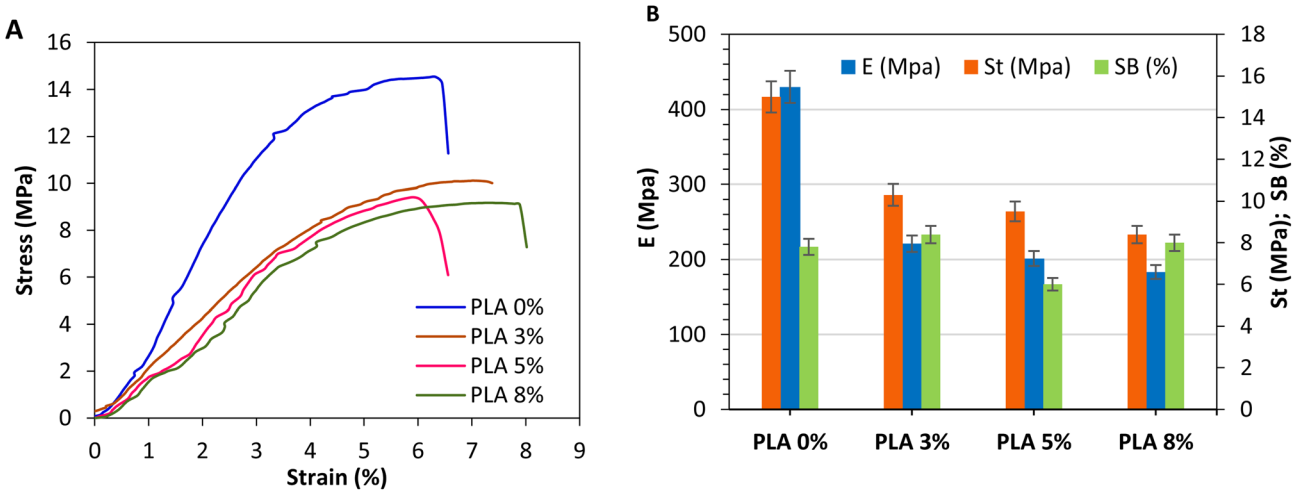

Fig. 1 (A) Stress–strain plots, and (B) strength (*S*), Young's modulus (*E*), and strain at break (SB) of neat PLA and plasticized PLA/OLE films with different OLE contents.

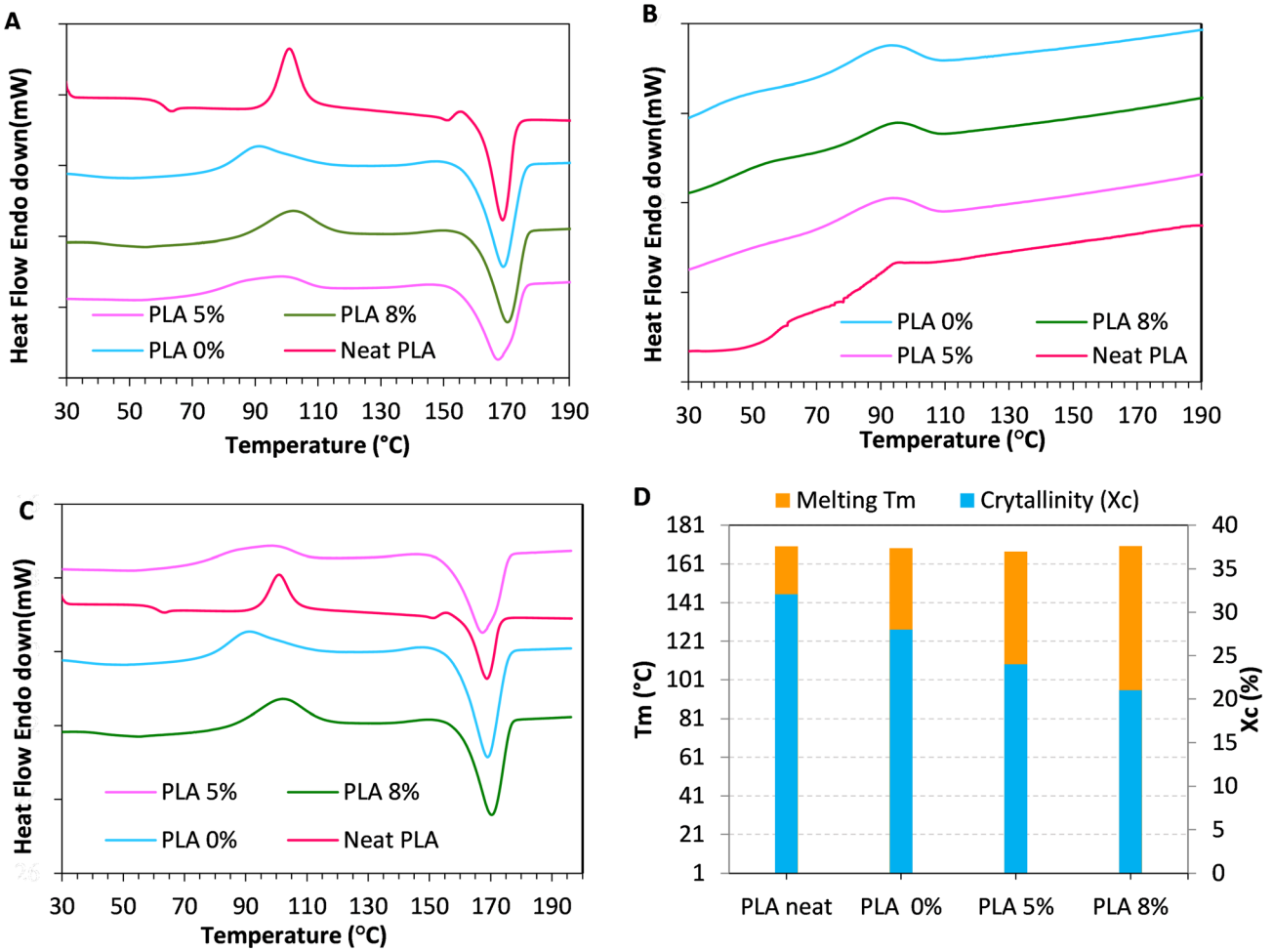

Fig. 2 DSC analysis data: (A) first heating scans, (B) cooling plots, (C) second heating scans, and (D) melting temperature and degree of crystallinity X_c after the first and second scans of neat PLA, PLA 0%, PLA 5% and PLA 8%.

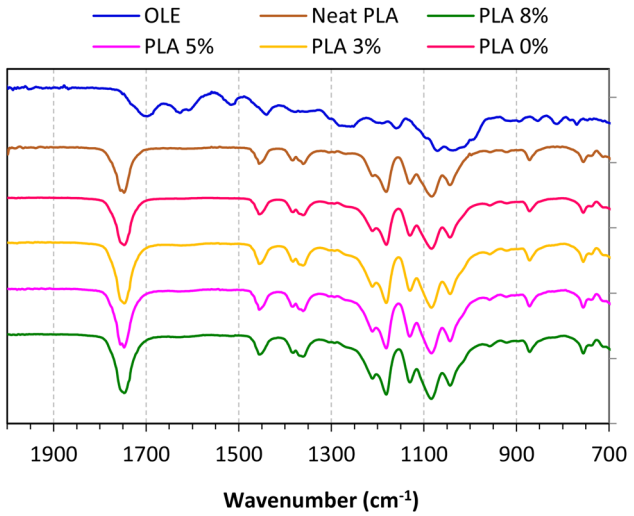

Fig. 3 FTIR spectra of OLE and PLA/OLE composite films.

or intensities, compared to plasticized PLA. One possible reason for this similarity is the relatively low concentration of OLE, which may be insufficient to induce detectable modifications in the FTIR spectra. Another possible explanation is the absence of strong physical interactions between OLE and PLA, which would otherwise cause shifts in certain FTIR band positions.

The visual characteristics of the PLA and PLA/OLE composite films are illustrated in Fig. 4. Neat PLA and PLA 0% films exhibit a bright, transparent appearance with no discernible color.

As the olive leaf extract is added, the films gradually take on a yellowish tint that becomes more pronounced at higher concentrations. Despite this color shift, the composite films remain translucent, allowing for a clear view through to the other side. As illustrated in Fig. 4, the neat PLA and the PLA 0% film exhibited high L^* (lightness) and a^* (red-green axis) values, while displaying low b^* (yellow–blue axis) values. The incorporation of olive leaf extract (OLE) resulted in a decrease in both L^* and a^* values, alongside an increase in b^* values. Consequently, the total color difference (ΔE) increased with the increasing

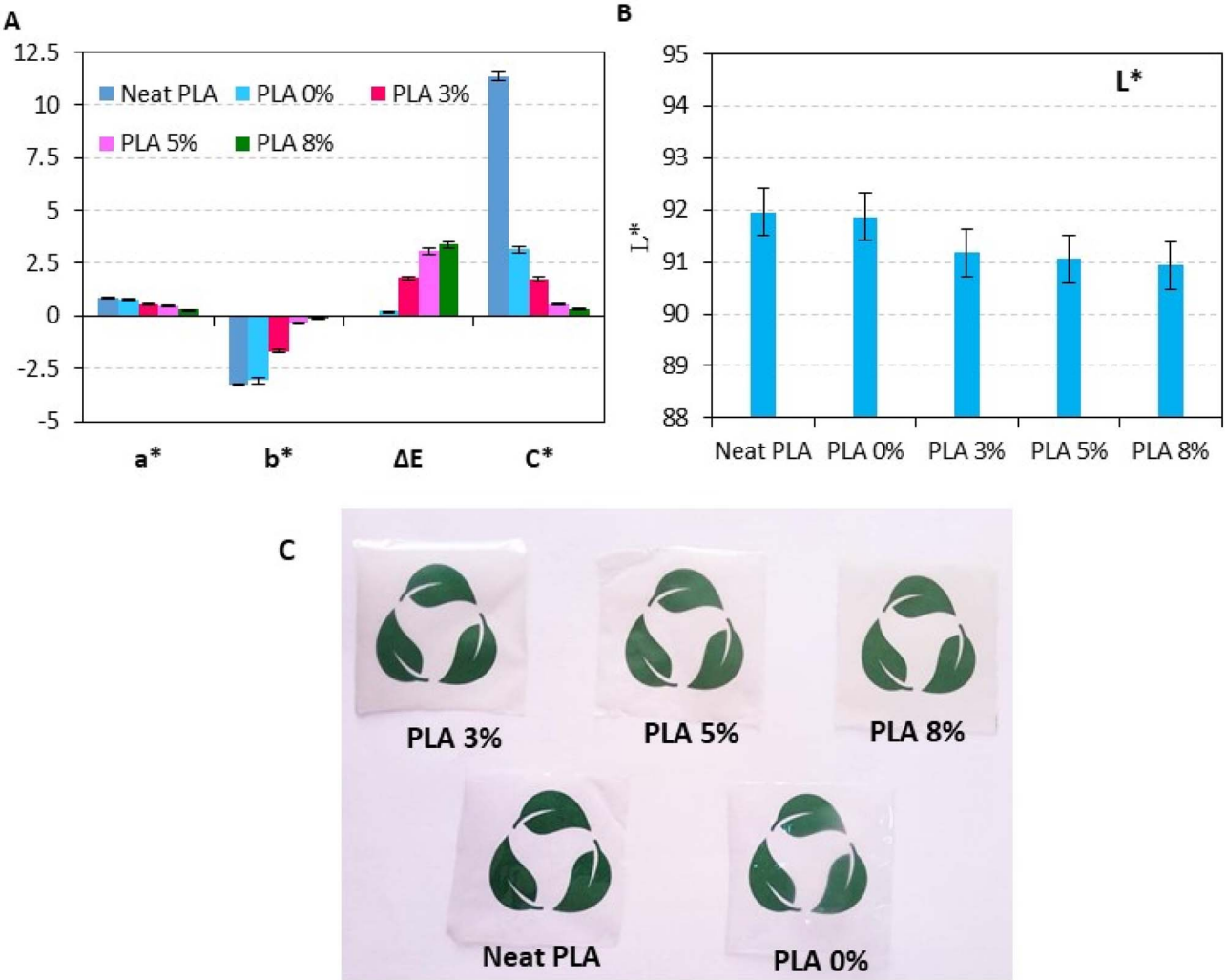

Fig. 4 (A and B) Color coordinates, and (C) visual images of the neat PLA, PLA 0% and PLA–OLE-based films.

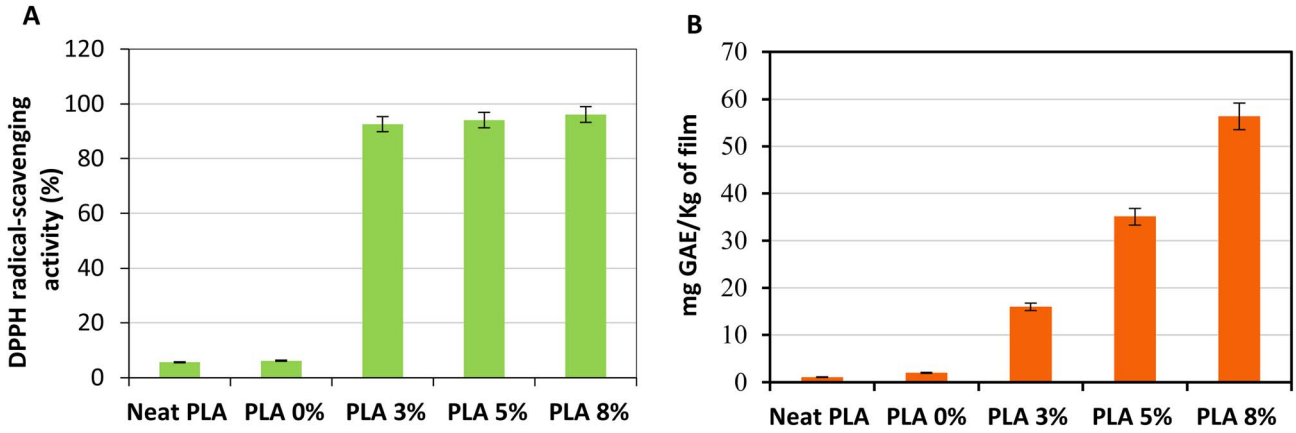

Fig. 5 Antioxidant potentials of PLA–OLE films with different concentrations by DPPH assay (A) and total antioxidant capacity test (B).

concentration of OLE extract. This can be attributed to the enhanced greenness and yellowness, resulting from the chlorophyll and phenolic compounds present in the OLE.

2.2.1 Antioxidant activity of the PLA–OLE films. The antioxidant properties of the PLA/OLE films were evaluated using two complementary methods: DPPH radical scavenging activity and TAC assay. The DPPH method measures an antioxidant's ability to neutralize the DPPH radical by donating a hydrogen atom.[31] As shown in Fig. 5A, neat PLA and PLA 0% films exhibited poor antioxidant activity, with low radical scavenging activity (RSA) values of approximately 5–6%. However, the incorporation of OLE extract led to a substantial increase in RSA (Fig. 5A), exceeding 92% even at an OLE concentration of 3% and reaching nearly 100% for the PLA 8% film. Interestingly, no significant difference in the antioxidant activity was observed between the 3%, 5%, and 8% OLE films, suggesting that a 3% OLE concentration is sufficient to achieve near-maximal antioxidant activity.

Fig. 5B shows the total antioxidant capacities (TAC) of the different PLA-based films, expressed in mg GAE/kg of the film, which are used to assess the ability of the films to reduce Mo(VI) to Mo(V) by acting as electron donors. The results indicate a significant enhancement in antioxidant activity with increasing OLE content, reaching a maximum of 55 mg GAE/kg of the film for PLA 8%.

These findings confirm the high efficiency of OLE in imparting antioxidant properties to PLA films. This antioxidant effect is attributed to the high phenolic content of OLE, which is well-documented for its strong radical scavenging and metal-reducing capabilities.[32]

2.3 Antibacterial efficiency of composite films

The antibacterial properties of the different composite films were also evaluated against different bacterial strains using agar diffusion methods. Table 2 shows the antibacterial activity of film samples against two Gram-positive bacteria (*Staphylococcus aureus* and *Listeria* sp.) and four Gram-negative bacteria (*Escherichia coli*, *Klebsiella pneumoniae*, *Salmonella enterica* and *Salmonella typhimurium*) strains by using the inhibitor zone determination.

As shown in Table 2, the prepared composite films showed varying degrees of antibacterial activity against all the tested bacterial strains. Furthermore, neat PLA films showed the lowest antibacterial effect against the most studied bacterial strains.

In addition, it was observed that the bacterial inhibitor activity showed a relative increase with the OLE extract amount incorporated into the prepared films. The results revealed enhanced antibacterial activity with higher amounts of OLE

Table 2 Antimicrobial activity of PLA/OLE films against different bacteria strains[a]

	Inhibition zone diameters (mm)				
Indicator organisms	Neat PLA	PLA 0%	PLA 3%	PLA 5%	PLA 8%
Gram (+)					
S. aureus	12.0 ± 0.5	13.0 ± 0.5	14.50 ± 0.6	15.0 ± 0.5	16.0 ± 0.5
Listeria sp.	8.0 ± 0.5	12.5 ± 0.6	15.0 ± 0.5	15.5 ± 0.5	15.5 ± 0.5
Gram (−)					
E. coli	10.0 ± 0.5	12.5 ± 1	13.0 ± 0.5	16.0 ± 0.5	14 ± 0.5
S. enterica	10.0 ± 1.5	12.0 ± 0.5	13.0 ± 0.5	15.0 ± 0.25	14.5 ± 0.5
S. typhimurium	11.0 ± 0.5	12.5 ± 0.65	13.0 ± 0.5	15.0 ± 0.25	15.0 ± 0.5
K. pneumoniae	10.0 ± 0.5	14.0 ± 0.5	15.0 ± 0.7	15.0 ± 0.5	15.5 ± 0.5

[a] The values are given as mean ± standard deviation. Gram +: Gram-positive bacteria strains. Gram −: Gram-negative bacteria strains.

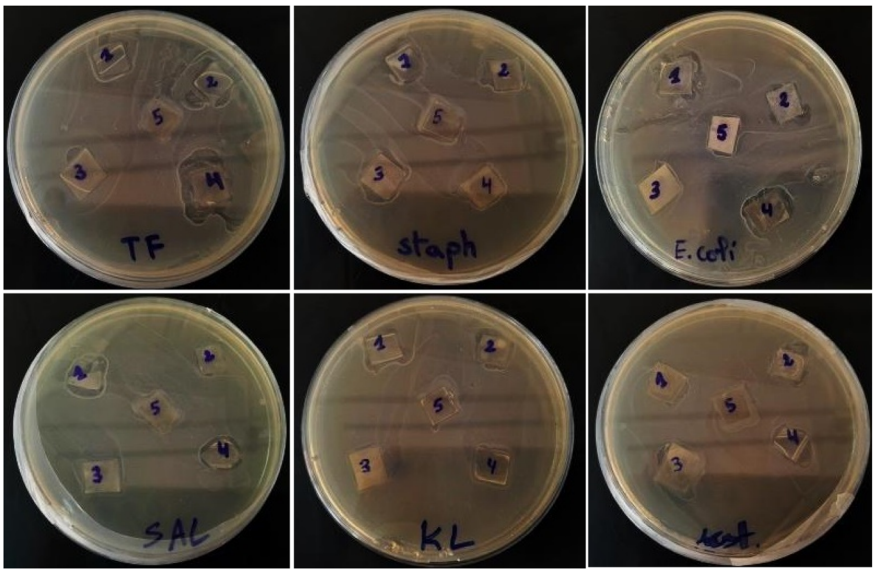

Fig. 6 Representative photographs showing antimicrobial activities of PLA/OLE films against different bacteria strains (B): Kl: *K. pneumoniae, E. coli,* SAL: *S. enterica,* Staph: *S. aureus,* TF: *S. typhimurium* and List: *Listeria* sp.

extract (5 and 8%), particularly against *Listeria* sp., *S. aureus* and *K. pneumoniae* (15–16 mm) (Fig. 6).

The biological properties of the composite films based on PLA and OLE extract against the different bacteria strains (Gram + and Gram −) were also dependent on the phenolic composition, their structure and the hydroxyl group (number and position).[33]

The antimicrobial mechanism of the films might be due to the adsorption onto the surfaces of microbial cells, the cytoplasmic membrane binding, which inhibited the transport of essential nutrients into the bacterial cells. Therefore, the physiological activities of the bacteria were inhibited, leading to a reduction in bacterial viability.[34]

2.4 Migration extent of OLE

2.4.1 Total phenolic migration test. The evaluation of the stability of PLA/OLE-based films through the migration of phenolic compounds was conducted using three food simulants: A, B, and D1. The migration test aimed to quantify the total amount of phenolic compounds that could transfer from the films into food products over time. The results are presented in Fig. 7, indicating that the migrated phenolic amounts increased with time and with increasing concentrations of OLE. Comparing the three OLE contents, it can be seen that at 3% and 5% OLE in PLA films, the total migrated phenolic compounds after 21 days remained lower than the critical threshold level of 60 mg kg^{-1}; according to the EC 2011, the critical threshold should not be exceeded for safety. At 8% OLE content, the level of total migrated phenolic compounds exceeded 70 mg kg^{-1} for simulants B and D1. While an overall migration assessment was not conducted, it is important to emphasize that olive leaf extract (OLE) is a natural extract, widely reported as safe and non-toxic, with its major compounds (oleuropein and hydroxytyrosol) evaluated and recognized as safe by EFSA and the US FDA. Considering these aspects, together with the relatively low migration values obtained for PLA films, the developed PLA/OLE films can reasonably be regarded as compliant with food-contact material regulations.[35–37]

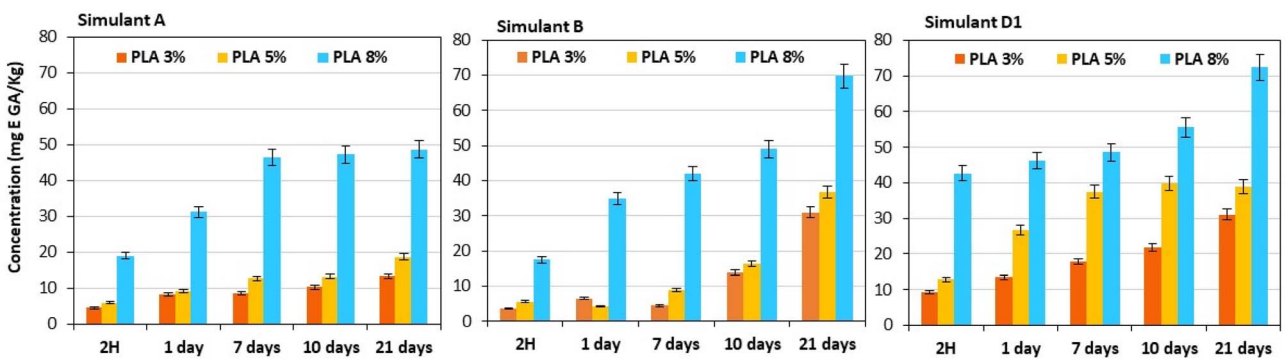

Fig. 7 Total phenolic compounds migrated into different food simulants A, B and D1.

2.4.2 Specific migration test. HPLC-DAD analysis was performed to identify and quantify migrating phenolic compounds from PLA 8%, based on a database of standard phenolic compounds. Migration testing was conducted using three types of simulants as per EU regulations: simulant A, representing aqueous foods; simulant B, representing acidic foods; and simulant D1, representing alcoholic and fatty foods.

The results, shown in Fig. 8, indicate that migration levels vary significantly depending on both the type of simulant and the specific phenolic compound. Notably, simulant A exhibited the lowest migration, with most compounds being detected at very low or even undetectable levels, except for cinnamic acid, which showed a notable increase over time. Oleuropein was not detected in any of the simulants, likely because it hydrolyzed into hydroxytyrosol. This explains the high levels of hydroxytyrosol observed across all simulants.

Moderate migration was noted in simulant B, especially for hydroxytyrosol, which reached its peak migration rate of 97.0 μg mL^{-1} after 15 days. This suggests that the acidic environment may enhance the release and mobility of hydroxytyrosol, potentially improving its antioxidant properties in food products. Rutin showed significant concentrations on day 1, but its levels decreased by day 15, indicating possible degradation over time.

The highest migration levels were observed in simulant D1, reaching 97.0 μg mL^{-1} for hydroxytyrosol and 56.0 μg mL^{-1} for catechin after 15 days. Interestingly, triacetin showed lower migration levels compared to the phenolic compounds. Its concentrations increased slightly over time, indicating its high stability across the three simulants. It is important to note that triacetin is a commonly used plasticizer in food packaging, pharmaceuticals, cosmetics, and tobacco products. It is considered to have low toxicity and is generally recognized as

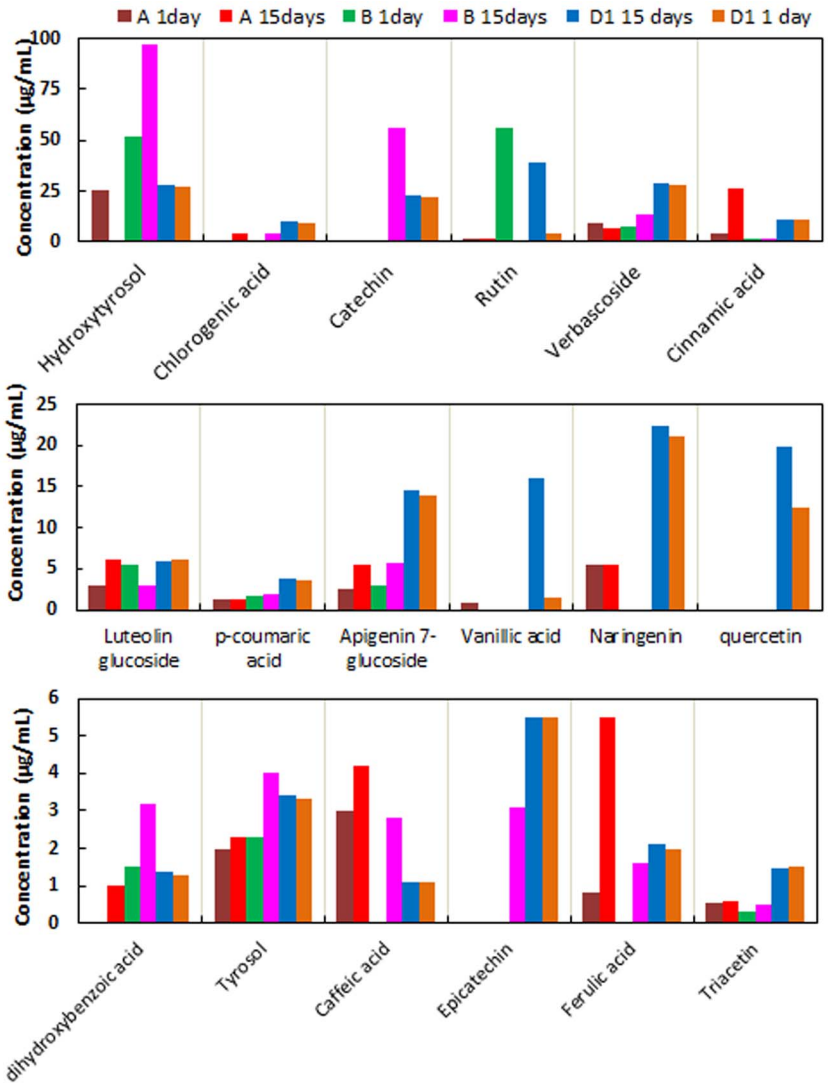

Fig. 8 Identification and quantification of migrated phenolic compounds and triacetin from PLA 8% film into different food simulants based on HPLC-DAD analysis.

safe (GRAS) by regulatory agencies such as the US FDA and EFSA.[38–40]

2.5 Degradation behavior of the PLA–OLE films

To evaluate the biodegradability of our materials, we conducted a disintegration test under burial conditions, monitoring both physical fragmentation and CO- release.

2.5.1 Disintegration under burial conditions. The macroscopic changes in the films over 40 days of burial in a controlled soil simulant at 58 °C are shown in Fig. 9A. All samples progressively disintegrated, and by the end of the test period, most of the film had fragmented, leaving only small residual debris. However, when comparing the sensitivity to fragmentation, it appears that the presence of OLE (≥5%) enhances disintegration. As shown in Fig. 9A, films containing 6% and 8% OLE underwent severe disintegration, whereas the neat PLA (0% OLE) remained largely intact, displaying coarse fragments.

A remarkable change in the color of the incorporated films was also observed. PLA/OLE-based films become more yellowish, brownish and opaque, especially PLA 8% and PLA 5%, due to their high amount of phenolic acids, which increased throughout the composting period, due to the promotion of the oxide.[41] These phenolic acids reduce the pH of the compost environment, thereby facilitating hydrolytic and microbial activity, which accelerates the biodegradation process.[42]

2.5.2 Biodegradation rate determined using carbon mineralization. To further evaluate the biodegradation potential of the PLA–OLE films, we measured the amount of CO- produced through the mineralization of carbon in various PLA samples. The results, illustrated in Fig. 9B, present the biodegradation percentages of neat PLA, PLA 0%, and PLA 8% composite films after 60 days of incubation at 58 °C. For all samples, a lag phase was observed before degradation

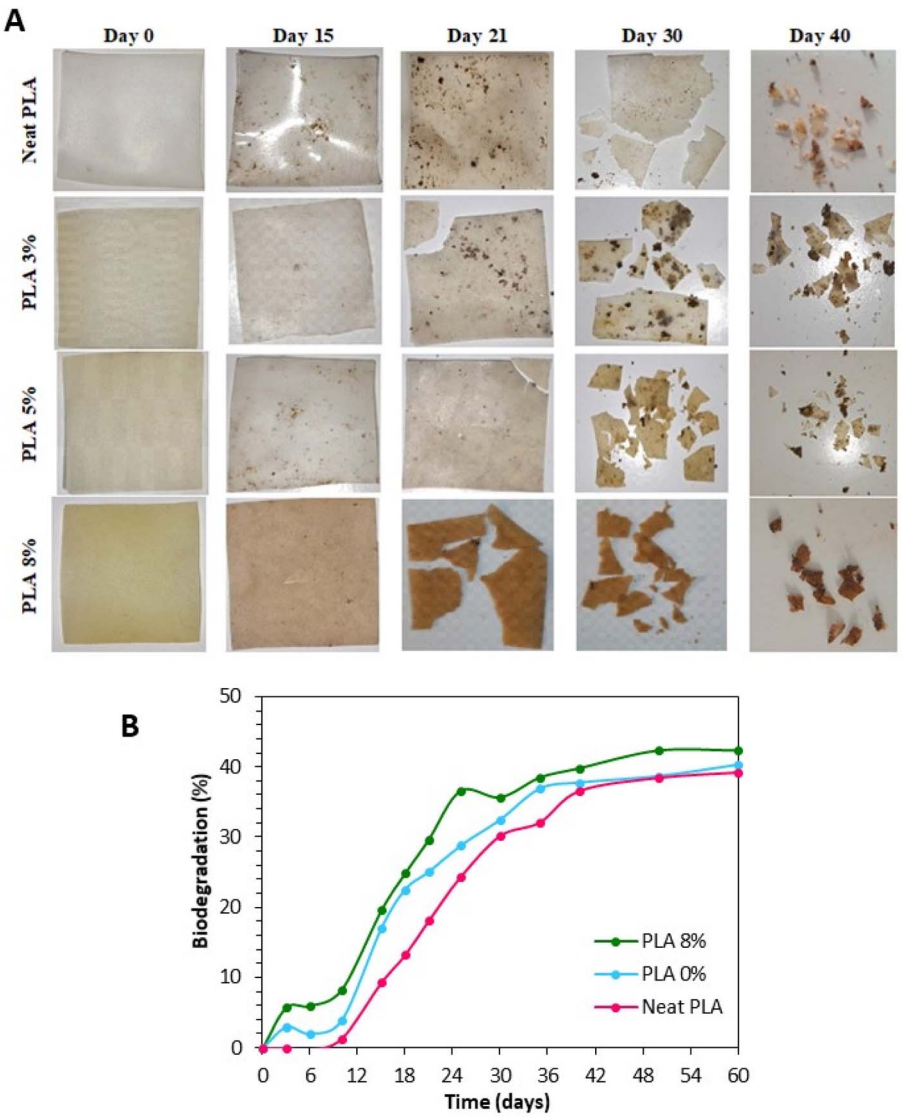

Fig. 9 (A) Visual images of the films after different times of burial in soil. (B) Biodegradation test of neat PLA, PLA 0%, PLA 8% films based on the mineralization of carbon at 58 °C.

commenced, continuing until a plateau was reached at approximately 40% after 35 days. This initial lag phase may be attributed to the time required for microbial communities in the compost to adapt to their new environment.[43] Among the samples, PLA 8% exhibited the highest biodegradation, reaching nearly 43%. Plasticized PLA (PLA 0%) also showed improved biodegradation compared to neat PLA, though at a slightly lower rate than PLA 8%. In contrast, neat PLA degraded the slowest, achieving only 39% by the 60th day. The enhanced biodegradation observed in PLA 8% can be attributed to the presence of 8% OLE, which serves as an effective carbon source for microbial growth. This is likely due to the low molecular weight of OLE phenolics, which act as substrates for enzymatic hydrolysis.[44] These findings align with previous research that reported a similar biodegradation profile for PBAT/PLA blends, achieving comparable results at 58 °C after 60 days of testing.[45] Based on the above analysis, it is evident that the addition of OLE did not compromise the biodegradability or compostability of the PLA film. This outcome is expected given OLE's biobased origin and its chemical composition, which consists of phenolic compounds known for their susceptibility to enzymatic biodegradation.

2.6 Application for cherry tomato preservation

Cherry tomatoes are climacteric, short-season fruits with high perishability and a reduced shelf life due to their elevated respiratory metabolism, which is influenced by their high moisture content.

The potential of PLA–OLE films in extending the shelf life of cherry tomatoes was assessed through a cold storage experiment. Fruits were packed in PLA films enriched with different amounts of OLE extract (PLA 0%, PLA 5%, and PLA 8%). The fungal decay index, calculated as the infected sample percentage relative to total packed fruits, was monitored throughout cold storage and compared to unpacked control samples. As shown in Fig. 10A, at day 21, a significant difference was detected depending on the packaging composition. The control group (unpacked fruits) exhibited signs of rotting, as did fruits packed in the PLA film without OLE (PLA 0%). In contrast, cherry tomatoes stored in PLA–OLE films maintained their vibrant appearance and remained free from rot up to day 21 for PLA 3%, 5%, and 8%. The best preservation effect was observed in fruits packed in PLA 5% and PLA 8%, which remained resistant to spoilage for up to 30 days. This trend is clearly depicted in Fig. 10B, which illustrates the change in the fungal decay index over time. By the 7th day of storage, the fungal decay percentages of unpacked cherry tomatoes showed a significant increase to 10%, whereas they remained at only 4% for PLA–OLE-coated fruits. Throughout cold storage, the fungal decay index of cherry tomatoes packed in PLA enriched with OLE extract (3–8%) increased gradually but remained lower than that of the uncoated samples. By the 21st day, the results show a significant reduction in fungal decay percentages for cherry tomatoes packaged in PLA enriched with 5% and 8% OLE, with decay

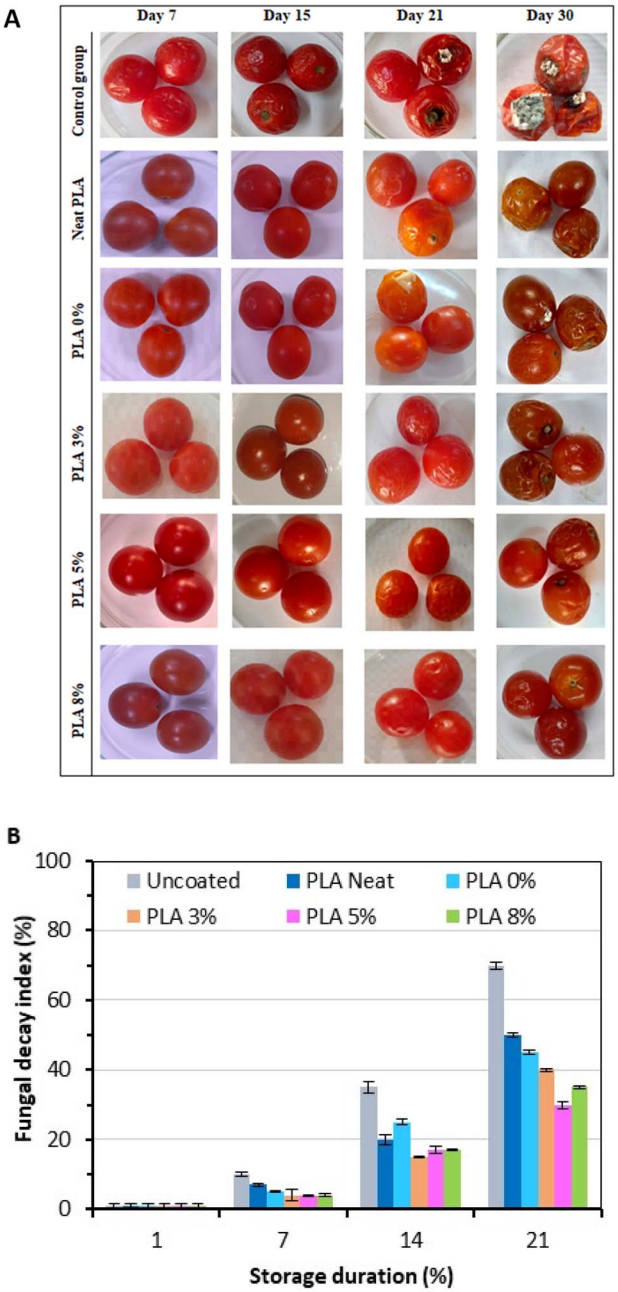

Fig. 10 Appearance quality (A) and fungal decay index (B) of cherry tomatoes uncoated and coated with neat PLA, PLA 0% and PLA–OLE composite films.

rates of 30% and 35%, respectively, compared to 70% for unpacked samples ($p < 0.05$).

This suggests that PLA–OLE film packaging is effective in extending the shelf life of cherry tomatoes, maintaining their quality for 21 days of cold storage. The improved storage quality and increased resistance to fungal decay can be attributed to the antimicrobial properties of the OLE extract.[46] The biodegradable composite films enriched with olive leaf extract exhibit a remarkable ability to prevent food spoilage by regulating fruit respiration and suppressing the growth of microorganisms on

Table 3 Change of the pH values of the uncoated and coated cherry tomatoes during cold storage at 4 °C

Day	Unpacked	Neat PLA	PLA 0%	PLA 3%	PLA 5%	PLA 8%
1	4.32 ± 0.022	4.4 ± 0.01	4.7 ± 0.12	4.3 ± 0.08	4.5 ± 0.15	4.6 ± 0.02
7	4.25 ± 0.02	4.37 ± 0.028	4.78 ± 0.084	4.28 ± 0.056	4.61 ± 0.084	4.59 ± 0.017
14	3.28 ± 0.4	4.75 ± 0.07	4.845 ± 0.01	4.855 ± 0.01	4.485 ± 0.02	4.53 ± 0.014
21	3.405 ± 0.05	4.845 ± 0.012	4.935 ± 0.01	4.815 ± 0.02	4.56 ± 0.015	4.4 ± 0.042

the fruit's surface.[47] This capacity for preservation is consistent with the findings of Zhao *et al.*,[48] which demonstrated that similar PLA-based films displayed high antibacterial activity against *E. coli* and *S. aureus*, effectively reducing their populations by 63.5% and 68.9%. These films proved highly effective in the prevention of microbial growth when used as antimicrobial food packaging for poultry products, and resulted in the extension of the shelf life of fresh chicken breast up to 8 days.

2.6.1 pH, weight loss rate and titrable acidity. The pH changes of cherry tomatoes during cold storage were investigated, and the results are shown in Table 3. It can be seen that on the 1st day, the pH values of cherry tomato juice were in the range of 4.32 to 4.85 for the six groups. Overall, the cherry tomatoes packaged in PLA films had a higher pH compared to the unpacked ones (control group). Notably, the pH of the cherry tomatoes packed in PLA–OLE 5% and 8% films remained at 4.4 and 4.56 throughout the cold storage (14th and 21 days), suggesting a relatively fresh state of the packaged fruits. However, the pH values were significantly decreased at lower levels (pH: 3.28–3.4) for uncoated samples.

As observed, both PLA–OLE composite films were effective in maintaining the pH values of fruit during storage for 21 days, as compared to the uncoated samples. Furthermore, the variation of the pH was also attributed to the microbial contamination, metabolite production by fungi and bacteria on the cherry tomato surfaces, and the presence of acidic autolysis compounds, as pH is decreased with increasing CFU g^{-1} values. It was observed that the PLA films and especially the PLA/OLE packaging maintained the pH for 21 days, as compared to the unpacked samples. Based on these observations, it can be concluded that PLA/OLE packaging was also effective in extending the shelf life of cherry tomatoes during cold storage.

The weight changes were an essential parameter for the quality evaluation of the cherry tomatoes during storage. The post-harvest fruit loss of water was also attributed to the respiration and transpiration of fruits, and caused the appearance of degeneration symptoms (shrinkage and brilliance losses). The weight loss percentages of the cherry tomatoes are shown in Fig. 11A. The results showed that fruit weight loss increased significantly in all unpacked and packed groups during storage, whereas the PLA–OLE composite packaging limited this increase.

On the 7th day, the weight loss percent was 2–2.5% for coated fruits with PLA–OLE composite films, significantly lower than the unpacked group (6.5%). PLA–OLE (5 and 8%) packaging improves the cherry tomato weight with at least a three-fold decrease in the weight loss percent. Respiration is one of the most important physiological metabolisms of fruits and reflects the dissipative speed of the inclusion of tissue. The respiration rate of the fruits gradually reduced during storage, which was consistent with the respiration pattern of uncoated fruits.

After the storage (14, 21 days), a significant weight loss percentage reduction could clearly be seen, from 10% to 3–4% for unpacked and packed tomatoes with PLA/OLE films, respectively. This observation was due to the formation of an extra layer around the fruits, which reduced the transpiration rate and therefore the weight loss. The olive leaf extract

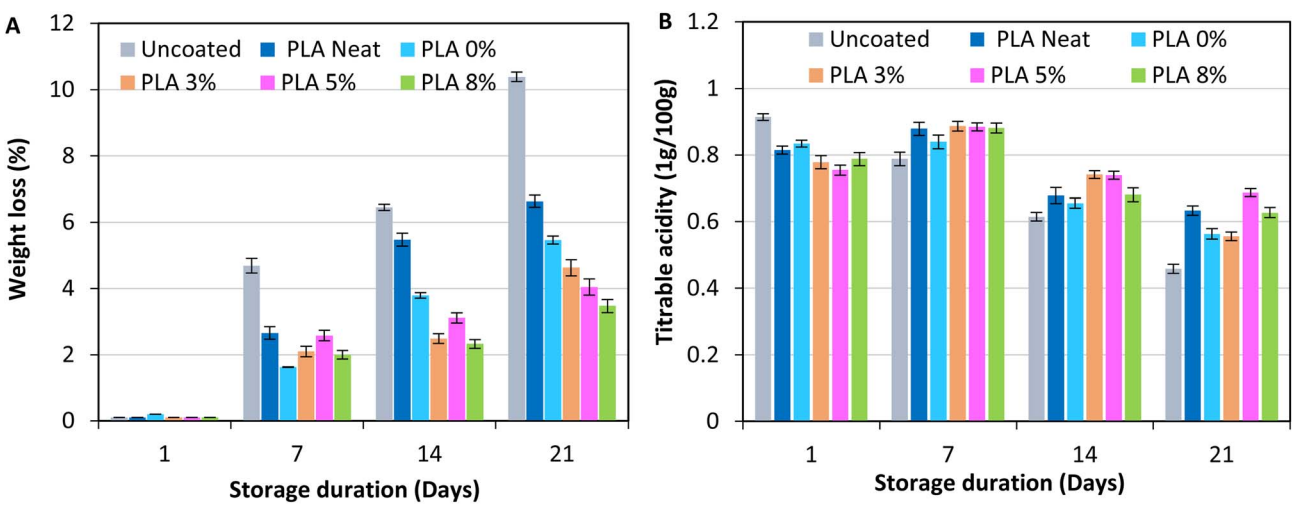

Fig. 11 The weight loss (A) and titrable acidity content (B) of cherry tomatoes uncoated and coated with PLA–OLE composite films.

incorporation of the composite films improves the coacervation of the fruits due to their chemical composition being enriched with different bioactive compounds, terpenes, flavonoids, sterols and polyphenols,[10–12] due to their hydrophobic character and antioxidant and antimicrobial properties. The results were in line with a previous study,[21] which showed that olive leaf water/ethanol extract could be used as an antioxidant and antibacterial ingredient in gelatin-based films for effective preservation of cold fish.

The results showed that the PLA film enriched with OLE extract was effective as a physical barrier to moisture loss, and to dehydration and cherry tomato deterioration. The application of biodegradable packaging of fruits promoted the covering and filling of lenticels and stomata, then reduced the transpiration (moisture transfer) and the respiration (exchanges of gas), which enhanced and extended the shelf life of the fruits .[49,50]

Cherry tomatoes are functional foods that are enriched with antioxidant products, such as vitamin C, fiber, lycopene and phenolic compounds, as well as citric and malic acids. Therefore, the citric acid amount was also determined for the different cherry tomato groups. Fig. 11B presents the titrable acidity of different conserved fruits during 21 days of storage at 4 °C. A notable decrease in the citric acid concentration can be observed, which can probably be attributed to the consumption of organic acids in the process of respiration.

The titrable acidity on the 1st day was 0.7–0.9% for the uncoated sample and PLA enriched with OLE extract. These results are higher than those cited previously[51] (0.45–0.55%). After storage, the titratable acidity was affected for the unpacked and packaged fruits. After 21 days, the unpacked fruits have the lowest titratable acidity as compared to the other films (PLA–OLE 5% and PLA–OLE 8%), thus, PLA films enriched with OLE extract resulted in a titrable acidity retention of cherry tomatoes during 21 days of storage.

PLA–OLE packaging reduced the fruit maturation, and the pH and titratable acidity were significantly lower than in the unpacked cherry tomatoes. Therefore, the biodegradable films were efficient for preserving the shelf life and quality of tomatoes, and can be used as antimicrobial packaging materials. The observations were in accordance with previous reports.[52,53] A titratable acidity decrease was shown for further fruit ripening during storage. This could be a result of the bacterial contamination, molds and yeast of the fruit, which accelerated citric acid loss.

2.6.2 Microbiological analysis. During cold storage, the microbial contamination of cherry tomatoes was also recognized. Therefore, yeast, mold, and mesophilic and psychrophilic bacteria plate counts were also investigated. The mold and yeast counts were 0.31 log CFU g^{-1} on the 1st day, which represented an acceptable fruit quality rating (Table 4). After 7 days of cold storage, the mold and yeast count values increased to 3.09 log CFU g^{-1} for unpacked cherry tomatoes as compared to PLA–OLE packed fruits (1.6 to 2.6 log CFU g^{-1}). After 21 days, the highest mold and yeast counts were observed for the unpacked samples (4.09 log CFU g^{-1}), compared to 3.25 and 2.31 log CFU g^{-1} for the coated cherry tomatoes with neat PLA and PLA 8%, respectively. Thus, PLA–OLE packaging could significantly reduce the rate of infection of the fruits, as compared to unpacked ones after cold storage duration.

Mesophilic and psychrophilic bacteria were additionally studied, and the results showed a similar trend to that of the molds and yeast (Table 4). In particular, at 14 days, the mesophilic and psychrophilic bacteria populations were 2.9 and 3.18 log CFU g^{-1}, for the unpacked groups, respectively. Furthermore, the results were lower for PLA 8% coated fruits (2.39 and 2.5 log CFU g^{-1}, respectively), which indicated lower bacterial contaminations of the cherry tomatoes. It can be concluded that the use of PLA enriched with OLE extract (as an antimicrobial and antioxidant compound) in the packaging could be a novel way to improve the safety of cherry tomatoes during cold storage, without using synthetic compounds. These results were in line with a previous study,[48] which reported that PLA-based

Table 4 Mold, yeast and bacteria plate counts of cherry tomatoes during cold storage

Treatments/storage time		Day 1	Day 7	Day 14	Day 21
Yeast and molds	Uncoated	0.31 ± 0.02	3.09 ± 0.05	3.2 ± 0.021	4.09 ± 0.3
	Neat PLA	0.31 ± 0.02	2.64 ± 0.25	2.85 ± 0.04	3.25 ± 1.7
	PLA 0%	0.31 ± 0.02	2.62 ± 0.17	2.6 ± 0.378	3.09 ± 2
	PLA 3%	0.31 ± 0.02	2.15 ± 0.5	2.23 ± 1.02	2.3 ± 3.6
	PLA 5%	0.31 ± 0.02	1.66 ± 0.36	1.78 ± 1.56	2.17 ± 1.7
	PLA 8%	0.31 ± 0.02	1.6 ± 0.19	1.76 ± 0.76	2.31 ± 2.78
Mesophilic bacteria	Uncoated	1.124 ± 0.05	2.66 ± 0.2	2.9 ± 0.14	3.04 ± 0.7
	Neat PLA	1.124 ± 0.05	2.534 ± 0.25	2.83 ± 0.25	2.82 ± 0.4
	PLA 0%	1.124 ± 0.05	2.25 ± 0.07	2.52 ± 1.56	2.66 ± 0.1
	PLA 3%	1.124 ± 0.05	2.47 ± 0.15	2.74 ± 0.8	2.68 ± 0.14
	PLA 5%	1.124 ± 0.05	2.30 ± 0.25	2.47 ± 1.6	2.41 ± 0.78
	PLA 8%	1.124 ± 0.05	2.20 ± 0.35	2.39 ± 0.9	2.34 ± 0.12
Psychrophilic bacteria	Uncoated	1.18 ± 0.15	3 ± 0.18	3.18 ± 1.5	3.18 ± 0.07
	Neat PLA	1.18 ± 0.15	2.68 ± 0.2	2.7 ± 0.9	2.84 ± 0.4
	PLA 0%	1.18 ± 0.15	2.62 ± 0.05	2.89 ± 1.76	2.8 ± 0.23
	PLA 3%	1.18 ± 0.15	2.32 ± 0.02	2.72 ± 3.02	2.63 ± 0.09
	PLA 5%	1.18 ± 0.15	2.30 ± 0.1	2.4 ± 2.0252	2.35 ± 0.4
	PLA 8%	1.18 ± 0.15	2.27 ± 0.06	2.5 ± 0.8	2.36 ± 0.14

films were effective in microbial growth prevention and then used as antimicrobial packaging materials of foods, and could extend chicken coacervation up to 8 days.

3 Experimental

3.1 Preparation of olive leaf extract (OLE)

Fresh leaves of *Olea europaea* L. (Chemlali variety) were collected in January 2024 from Kasserine City, Tunisia, and taxonomically authenticated by Professor Khalil Messedi, botanist at the University of Sfax (Tunisia). A voucher specimen (code: LCSN 151 A) was prepared and deposited in the herbarium of the Laboratory of Organic Chemistry LR17ES08. The leaves were air-dried, powdered, and subjected to a two-step extraction process. First, 100 g of powdered leaves were extracted with 500 mL of hexane under constant stirring for 4 h at room temperature to remove chlorophyll and other non-polar constituents. The plant residue was then extracted with 500 mL of methanol for 24 h to recover secondary metabolites, particularly phenolic compounds. The methanolic extract obtained was filtered and concentrated under reduced pressure at 50 °C using a rotary evaporator, yielding the crude olive leaf extract (OLE).

3.2 Solvents and reagents

Polylactic acid (PLA) pellets (PLE 005-France) were purchased from NaturPlast-France. Chloroform, ethanol, methanol, hexane, acetic acid, and sodium carbonate of analytical grade were purchased from Merck (Darmstadt, Germany). Folin–Ciocalteu reagent and 2,2-diphenyl-1-picrylhydrazyl (DPPH) were obtained from Sigma-Aldrich (St. Louis, MO, USA). Triacetin (glyceryl triacetate, ≥99% purity) was purchased from Sigma-Aldrich. Authentic phenolic standards, including oleuropein, hydroxytyrosol, chlorogenic acid, catechin, rutin, verbascoside, cinnamic acid, luteolin-7-glucoside, *p*-coumaric acid, apigenin-7-glucoside, vanillic acid, naringenin, quercetin, dihydroxybenzoic acid, tyrosol, caffeic acid, epicatechin, and ferulic acid, were purchased from Sigma-Aldrich and used for calibration and compound identification.

3.3 Preparation of OLE/PLA-based films

The PLA films incorporated with methanolic olive leaf extract were prepared by dissolving 4% PLA in chloroform under constant stirring for 2 h. Subsequently, 20% of triacetin was added as a plasticizer, then different concentrations of olive leaf extract (3%, 5%, and 8% based on the total weight of PLA and plasticizer) were added, and the solutions were stirred until completely dissolved. Thin films with dry thicknesses of around 30–20 μm were obtained using film casting coaters with controlled thickness. The film was dried for 2 h at 60 °C. In the following, the film will be referred to as PLA X%, where X is weight percent of OLE in the dry film based on PLA and triacetin plasticizer.

3.4 Migration tests

To determine the migration of phenolic compounds, a migration test was conducted using three different food simulants: A (10% ethanol, v/v), B (3% acetic acid, w/v), and D1 (50% ethanol). Samples of 100 mg from each film were placed in the selected food simulants and incubated at 40 °C for various durations: 2 h, and 1, 7, 15, and 21 days. The amount of migrated phenolic compound was then measured using the Folin–Ciocalteu method, using gallic acid as the calibration standard.[22] Briefly, 1 mL of the liquid portion from each simulant sample was blended with 5 mL of diluted Folin–Ciocalteu reagent. After incubation for 5 min, 4 mL of 7.5% Na_2CO_3 was added. The mixture was then stored in the dark at room temperature for 2 hours. The absorbance was then measured at 765 nm, and the results were expressed in milligrams of gallic acid equivalent per kg of film (mg GAE kg^{-1}). All experiments were performed in triplicate.

To quantify and identify specific phenolic compounds and plasticizers that migrated from the PLA 8% film into the various simulants A, B, and D1 after 1 day and 15 days, HPLC-DAD analysis was performed. This analysis was carried out using an RP-C18 column (250 × 4.6 mm, 5 μm). The mobile phase consisted of water containing 0.1% formic acid (solvent A) and methanol (solvent B). A linear gradient elution was applied, starting from 5% B and reaching 100% B within 45 min, at a constant flow rate of 0.8 mL min^{-1}. The injection volume was 20 μL, and detection was performed with a diode array detector (DAD) at 280 and 320 nm. Phenolic compounds were identified primarily by direct comparison of their retention times and UV spectra with those of authentic reference standards (oleuropein, hydroxytyrosol, chlorogenic acid, catechin, rutin, verbascoside, cinnamic acid, luteolin-7-glucoside, *p*-coumaric acid, apigenin-7-glucoside, vanillic acid, naringenin, quercetin, dihydroxybenzoic acid, tyrosol, caffeic acid, epicatechin, and ferulic acid).

3.5 Color coordinates

The color parameters of the PLA/OLE-based films were measured using a Chroma Meter CR-400 colorimeter from Konica Minolta, INC (Japan). The instrument was calibrated using a standard white tile ($L^* = 95.09$, $a^* = -0.13$, and $b^* = 3.53$). Three color parameters were analysed: lightness (L^*), which represents the achromatic component of color and ranges from 0 (absolute black) to 100 (perfect white); saturation (a^*), which represents the chromatic component of color on the red-green axis, and finally, the tone angle (b^*), which represents the chromatic component of color on the yellow–blue axis (positive values indicate yellowness while negative values indicate blueness). These three parameters were utilized to determine the total color difference (ΔE), and chroma C^*, which indicated the color saturation, using the following equations (eqn (1) and (2)):

$$\Delta E = \sqrt{\Delta L^{*2} + \Delta a^{*2} + \Delta b^{*2}} \quad (1)$$

$$C^* = \sqrt{a^{*2} + b^{*2}} \quad (2)$$

where $L^{*'} = L^*_{\text{Neat}} - L^*_{\text{sample}}$; $a^* = a^*_{\text{PLA Neat}} - a^*_{\text{sample}}$ and $b^{*'} = b^*_{\text{Neat}} - b^*_{\text{sample}}$.

3.6 Structural and thermal properties

The FTIR measurements of the composite films were performed using a PerkinElmer spectrometer fitted with a single-reflection diamond crystal plate. The data were recorded at a resolution of 4 cm^{-1} across a range of 500 to 4000 cm^{-1}.

The thermal assessment of transition temperatures for PLA/OLE bioactive films, including glass-transition temperature (T_g), melting temperature (T_m), and the enthalpies of fusion (ΔH_m) and crystallization (ΔH_c), was conducted using a differential scanning calorimeter (DSC); DSC-6000 (PerkinElmer-Shelton-USA). About 5 mg of the film was sealed in an Al pan and analyzed between −10 to 200 °C, with a heating rate of 10 °C min^{-1} and under an N_2 atmosphere.

$$X_c\ (\%) = \frac{100 \times (\Delta H_m - \Delta H_{cc})}{\Delta H^0_m \times m_P} \quad (3)$$

The degree of crystallinity X_c was determined using eqn (3), where ΔH_m and ΔH_c correspond to the melting and cold crystallization enthalpies of the sample. Mp is the weight of the sample, and $\Delta H_m{}^0 = 93.1\ J\ g^{-1}$ is the melting enthalpy of 100% crystalline PLA.[54]

3.7 Mechanical properties

The mechanical properties of the PLA film samples, such as strength (S) and strain at break (SB), were assessed through tensile testing utilizing an INSTRON universal testing machine configured to a crosshead speed of 5 mm min^{-1}. Each PLA film sample was cut to dimensions of 2 cm × 4 cm, featuring an approximate gauge length of 3 cm.

3.8 Disintegration test

Square film samples of 2 cm^2 were buried approximately 4 cm deep in humid soil made up of vegetable compost at a temperature of 58 °C. Water was sprayed daily to maintain the moisture levels of the compost. PLA samples were carefully retrieved at various time intervals and captured to visually track the condition of the films.

3.9 Biodegradation test

The biodegradation test was conducted by measuring the amount of CO_2 produced due to the breakdown of PLA samples by soil microorganisms to determine the extent of biodegradation. A mixture of organic compost and soil in a 1 : 1 ratio was prepared, humidified, and used as the test medium. PLA samples were tested alongside a control (soil/compost without PLA film samples). PLA film pieces (4 cm × 4 cm) were weighed and placed at a depth of about 4 cm below the soil surface within the flasks, ensuring full contact with the soil on both sides. A beaker containing 30 mL of 0.05 mol L^{-1} KOH, serving as a CO_2 trapping solution, was placed in each flask. The flasks were then incubated at 58 °C.

To maintain the soil's moisture content above 70% throughout the test period, distilled water was regularly misted onto the soil. The CO_2 uptake by the KOH solution was measured at the end of each degradation period (3, 6, 10, 15, 18, 21, 25, 30, 35, 40, 50, and 60 days) by titrating the KOH solution against 0.001 mol L^{-1} HCl, using phenolphthalein as an indicator. The rate of biodegradation was assessed by plotting the percentage of released CO- over time according to eqn (4):

$$\text{Biodegradation}\ (\%) = \frac{\text{mCO}_2\ (\text{sample}) - \text{mCO}_2\ (\text{control})}{\text{ThCO}_2} \times 100 \quad (4)$$

$$\text{Th}_{\text{CO}_2} = \frac{44 \times M_T \times C_T}{12} \quad (5)$$

$$\text{mCO}_2 = V \times 22 \times C_{\text{HCl}} \quad (6)$$

where V, C_{HCl}, 44, Th_{CO2}, C_T, M_T, and 12 are the volume of HCl consumed, the concentration of HCl solution, the molar mass of CO_2, the theoretical carbon dioxide value, the relative amount of total carbon per total weight, the total weight, and the molar mass of C, respectively. Th_{CO2} and mCO_2 were calculated according to eqn (5) and (6).

3.10 Biological activities of the composite films

3.10.1 Antioxidant activity. To evaluate the antioxidant effect of bioactive PLA–OLE-based films, the DPPH assay was conducted using a previously described method.[55] Briefly, a 1 cm^2 sample of each composite film was weighed and immersed in 3.9 mL DPPH solution. The mixture was then incubated in a dark room for 120 min, with stirring every 30 min to ensure proper interaction. After incubation, the mixture was filtered, and the absorbance was recorded at a wavelength of 515 nm. The radical scavenging activity was determined as a percentage of DPPH inhibition using the following equation:

$$\text{DPPH radical scavenging activity}\ (\%) = [(\text{Abs}_{\text{sample}} - \text{Abs}_{\text{blank}})/\text{Abs}_{\text{blank}}] \times 100$$

where Abs_{blank} refers to the absorbance value of the DPPH solution without interaction with the film samples, and Abs_{sample} represents the absorbance of the DPPH solution after interacting with the tested film.

The total antioxidant capacity (TAC) of the PLA-based films was determined following a previously established method with slight modifications.[31] Briefly, 100 mg of each film sample was placed in ethanol for 2 h. Then, 0.3 mL of the ethanolic supernatant was combined with 3 mL of reagent solution containing 0.6 M sulfuric acid, 28 mM sodium phosphate, and 4 mM ammonium molybdate. The solution was incubated in a boiling water bath for 90 min. After cooling, the absorbance was recorded at 730 nm. The TAC was expressed in mg of gallic acid equivalents (GAE) per kg of film, based on a calibration curve prepared with standard solutions of gallic acid.

3.10.2 Antibacterial activity. The antibacterial activity of the composite films was investigated against several infectious bacterial strains using the disc agar diffusion method. The microorganisms used were two Gram-positive (*Staphylococcus aureus* ATCC 25923 and *Listeria* sp.) and four Gram-negative (*Escherichia coli* ATCC 25922, *Klebsiella pneumoniae* ATCC 13883, *Salmonella enterica* ATCC 43972 and *Salmonella typhimurium* ATCC 19430) samples, provided by the Center of Biotechnology, Sfax, Tunisia. A culture suspension (100 μL) of the tested microorganisms (about 10^6 colony-forming units) was spread over the Luria Bertani agar. Films (1 cm × 1 cm) were first sterilized by UV light for 30 min and then placed on the plate surfaces and incubated at 37 °C for 24 h. The antagonistic zones were detected after incubating at 37 °C for 24 h. The appearance of a clear zone below or around the films indicated the presence of antibacterial activity.

3.11 Application of PLA/OLE composite films for cherry tomato preservation

The cherry tomatoes were purchased from a domestic market in Sfax-Tunisia. For the present study, cherry tomatoes with a red color and an average weight of 10 ± 1 g (40–30 mm) were selected, and they did not have any visible mechanical damage or fungal infection.

The cherry tomatoes were sterilized for 5 min by immersing them in deionized water. Subsequently, the tomatoes were divided into six groups (6 cherry tomatoes for each group) as follows:

(1) the uncoated group (control) without any packaging film; (2) cherry tomatoes placed in neat PLA film; (3) cherry tomatoes placed in a bag from PLA 0% film; (4) cherry tomatoes placed in a bag from PLA 3% film; (5) cherry tomatoes placed in a bag from PLA 5% film; and (6) cherry tomatoes placed in a bag from PLA 8% film.

Six cherry tomatoes were placed in polypropylene plastic boxes for the different packaging samples (control and PLA-coated groups). The boxes measured 20.5 cm × 14.5 cm × 5.4 cm, with a thickness of 2.5 mm. They were stored at 4 ± 1 °C with a relative humidity of 95%. The different analyses were conducted after 7, 15, 21, and 30 days of cold storage.

3.11.1 Cherry tomato decay rates. The incidence of lesions, lesion expansion and mould contamination of cherry tomatoes during storage, was evaluated by the fruit percentages characterized by the presence of one or more white colonies or dark brown multicelled colonies. The results were expressed as infected fruit percentages compared to the initial fruits and determined as follows:

$$\text{Decay rate (\%)} = [\text{number of infected fruits/number of total fruits}] \times 100$$

3.11.2 pH, titratable acidity and weight loss. For the determination of pH and titrable acidity, cherry tomatoes from each coated and uncoated group were pressed with distilled water in a hand press, and the obtained tomato juice was used. The total titratable acidity was studied by titrating tomato juice (5 mL) to a pH of 8.1, by using a solution of 1 M NaOH. The total titratable acidity was expressed as grams of citric acid per 100 g of cherry tomatoes.

The weight loss is determined by the water loss, which was a vital factor for the quality evaluation of the conserved tomatoes. The weight loss percent (eqn (7)) was defined as the ratio of the final weight of the cherry tomatoes (W_1) to the initial weight (W_0) and was expressed as follows:

$$\text{Weight loss (\%)} = [W_0 - W_1]/W_0 \times 100 \quad (7)$$

3.11.3 Microbiological analysis. The bacteriological and fungal contamination of the conserved cherry tomatoes was evaluated using the pour plate technique. 1 g of each sample from the different conserved groups was put into sterile tubes and homogenized with 9 mL of sterile NaCl solution (0.9% w/v). Tenfold serial dilutions of tomato homogenates from this solution were carried out, and the resulting samples were used for bacterial and fungal determination. Total mesophilic and psychrophilic bacteria were determined using the plate count agar and then incubation at 37 °C and 4 °C for 1–3 days, respectively.

Yeast and mold counts were also conducted using the surface seeding technique with potato dextrose agar, incubated for 3–5 days at 30 °C. All microbial counts were reported as logarithms of colony-forming units per gram of cherry tomatoes (log CFU g^{-1}).

3.12 Statistical analysis

All experiments were conducted in triplicate, and the average values with standard deviations were reported. Statistical analyses were performed with SPSS ver. 17.0, professional edition, using ANOVA analysis. Differences were considered significant at $p < 0.05$. All tests were carried out in triplicate.

4 Conclusion

The incorporation of olive leaf extract (OLE) into PLA-based films enhances their antioxidant and antibacterial properties, making them ideal for eco-friendly food packaging. The compounds present in OLE, including oleuropein, flavonoids, and lignans, contribute to the improved performance of the films. The results indicate that adding OLE at 3%, 5%, and 8% concentrations increases the antioxidant activity and antibacterial effects of the PLA films. Additionally, mechanical and thermal property tests, as well as structural analysis by FT-IR, were conducted to further evaluate the characteristics of the resulting films. No effect of OLE on the chemical structure of the PLA/OLE films was detected. However, it enhanced mobility chains and improved their flexibility. The migration tests reveal that PLA/OLE films exhibit high stability and resistance to the migration of phenolic compounds, with most samples adhering to the legal limit of 60 mg kg^{-1} across various food simulants, including aqueous, acidic, and alcohol-containing solutions. The PLA films enriched with OLE have been proven to effectively

maintain safety and quality in food packaging. Coating cherry tomatoes with these films resulted in significantly lower fungal decay and better preservation of pH and acidity during 21 days of cold storage. This suggests that PLA/OLE coatings not only extend shelf life but also offer a safe and sustainable alternative to synthetic preservatives.

Author contributions

All authors made significant contributions to the manuscript. S. Soltani conducted the experiments and drafted the original manuscript. N. Allouche and S. Hajji contributed by developing the methodology and providing supervision throughout the research process. S. Boufi contributed to the conceptualization and methodology, as well as in writing and reviewing the manuscript, with support from all authors.

Conflicts of interest

There are no conflicts to declare.

Data availability

All raw data presented in this work are openly available in [zenodo] at: **https://doi.org/10.5281/zenodo.17448033**.

Acknowledgements

The authors gratefully acknowledge the Doctoral School of Fundamental Sciences at the Faculty of Sciences, Sfax University, for its support of this research project.

References

1 J. Wang, X. Yuan, S. Deng, X. Zeng, Z. Yu, S. Li and K. Li, *Green Chem.*, 2020, **22**, 6836–6845.
2 F. Serra-Parareda, M. Delgado-Aguilar, F. X. Espinach, P. Mutjé, S. Boufi and Q. Tarrés, *Composites, Part B*, 2022, **238**, 109901.
3 O. Alabi, K. Ologbonjaye, O. Awosolu and O. Alalade, *J. Toxicol. Risk Assess.*, 2019, **5**(2), 1–13.
4 Y. Hong, S. Wu and G. Wei, *Sci. Total Environ.*, 2023, **903**, 166258.
5 Z. Yuan, R. Nag and E. Cummins, *Sci. Total Environ.*, 2022, **823**, 153730.
6 H. Xu, Z. Hu, Y. Sun, J. Xu, L. Huang, W. Yao, Z. Yu and Y. Xie, *Environ. Geochem. Health*, 2024, **46**, 276.
7 X. Zhao, Y. Wang, X. Chen, X. Yu, W. Li, S. Zhang, X. Meng, Z.-M. Zhao, T. Dong, A. Anderson, A. Aiyedun, Y. Li, E. Webb, Z. Wu, V. Kunc, A. Ragauskas, S. Ozcan and H. Zhu, *Matter*, 2023, **6**, 97–127.
8 S. Nanda, B. R. Patra, R. Patel, J. Bakos and A. K. Dalai, *Environ. Chem. Lett.*, 2022, **20**, 379–395.
9 S. Sharma, K. Y. Perera, A. K. Jaiswal and S. Jaiswal, in *Food Packaging and Preservation*, Elsevier, 2024, pp. 133–152.
10 T. Michel, I. Khlif, P. Kanakis, A. Termentzi, N. Allouche, M. Halabalaki and A.-L. Skaltsounis, *Phytochem. Lett.*, 2015, **11**, 424–439.
11 A. Ghorbel, S. Wedel, I. Kallel, M. Cavinato, M. E. Sakavitsi, J. Fakhfakh, M. Halabalaki, P. Jansen-Dürr and N. Allouche, *J. Food Meas. Char.*, 2021, **15**, 1–14.
12 M. C. Dias, C. Figueiredo, D. C. Pinto, H. Freitas, C. Santos and A. M. Silva, *Ind. Crops Prod.*, 2019, **133**, 269–275.
13 G. S. da Rosa, S. K. Vanga, Y. Gariepy and V. Raghavan, *J. Polym. Environ.*, 2020, **28**, 123–130.
14 T. R. Martiny, V. Raghavan, C. C. de Moraes, G. S. da Rosa and G. L. Dotto, *Foods*, 2020, **9**, 1759.
15 T. R. Martiny, B. S. Pacheco, C. M. P. Pereira, A. Mansilla, M. S. Astorga-España, G. L. Dotto, C. C. Moraes and G. S. Rosa, *Food Sci. Nutr.*, 2020, **8**, 3147–3156.
16 S. Grabska-Zielińska, M. Gierszewska, E. Olewnik-Kruszkowska and M. Bouaziz, *Materials*, 2021, **14**, 7623.
17 C. Fiorentini, G. Leni, E. D. de Apodaca, L. Fernández-de-Castro, G. Rocchetti, C. Cortimiglia, G. Spigno and A. Bassani, *Antioxidants*, 2024, **13**, 519.
18 E. Musella, I. C. el Ouazzani, A. R. Mendes, C. Rovera, S. Farris, C. Mena, P. Teixeira and F. Poças, *Coatings*, 2021, **11**, 1339.
19 I. Khalifa, H. Barakat, H. A. El-Mansy and S. A. Soliman, *Food Biosci.*, 2016, **13**, 69–75.
20 M. Sabbah, A. Al-Asmar, D. Younis, F. Al-Rimawi, M. Famiglietti and L. Mariniello, *Coatings*, 2023, **13**, 1253.
21 I. Albertos, R. J. Avena-Bustillos, A. B. Martín-Diana, W.-X. Du, D. Rico and T. H. McHugh, *Food Packag. Shelf Life*, 2017, **13**, 49–55.
22 M. Moura-Alves, V. G. L. Souza, J. A. Silva, A. Esteves, L. M. Pastrana, C. Saraiva and M. A. Cerqueira, *Foods*, 2023, **12**, 4076.
23 A. B. Saad, M. Tiss, H. Keskes, A. Chaari, M. E. Sakavitsi, K. Hamden, M. Halabalaki and N. Allouche, *J. Diabetes Res.*, 2021, **2021**, 6659415.
24 I. Khlif, K. Jellali, T. Michel, M. Halabalaki, A. L. Skaltsounis and N. Allouche, *J. Chem.*, 2015, **2015**, 1–11.
25 K. Mnafgui, L. Ghazouani, R. Hajji, A. Tlili, F. Derbali, F. I. da Silva, J. L. Araújo, B. de Oliveira Schinoff, J. F. R. Bachega and A. L. da Silva Santos, *Neurochem. Res.*, 2021, **46**, 2131–2142.
26 N. Saadati Ardestani, A. Rojas, N. Esfandiari, M. J. Galotto, A. Babhadiashar and S. A. Sajadian, *Processes*, 2022, **10**, 1787.
27 S. Roy and J.-W. Rhim, *Int. J. Biol. Macromol.*, 2020, **162**, 1780–1789.
28 A. Torres, E. Ilabaca, A. Rojas, F. Rodríguez, M. J. Galotto, A. Guarda, C. Villegas and J. Romero, *Eur. Polym. J.*, 2017, **89**, 195–210.
29 V. A. I. Silveira, B. M. Marim, A. Hipólito, M. C. Gonçalves, S. Mali, R. K. T. Kobayashi and M. A. P. C. Celligoi, *Food Packag. Shelf Life*, 2020, **26**, 100591.
30 H. Sellami, S. A. Khan, I. Ahmad, A. A. Alarfaj, A. H. Hirad and A. E. Al-Sabri, *Int. J. Mol. Sci.*, 2021, **22**, 12562.
31 S. Soltani, I. Koubaa, I. Dhouib, B. Khemakhem, P. Marchand and N. Allouche, *Chem. Biodiversity*, 2023, **20**, e202200944.

32 I. Khlif, K. Jellali, T. Michel, M. Halabalaki, A. L. Skaltsounis and N. Allouche, *J. Chem.*, 2015, **2015**, 1–11.
33 M. Barbălată-Mândru, D. Serbezeanu, M. Butnaru, C. M. Rîmbu, A. A. Enache and M. Aflori, *Materials*, 2022, **15**, 2493.
34 J. Hasan and K. Chatterjee, *Nanoscale*, 2015, **7**, 15568–15575.
35 M. Monteiro, A. F. R. Silva, D. Resende, S. S. Braga, M. A. Coimbra, A. M. S. Silva and S. M. Cardoso, *Antioxidants*, 2021, **10**, 444.
36 EFSA Panel on Dietetic Products, Nutrition and Allergies (NDA), *EFSA J.*, 2011, **9**, 2033.
37 S. Granados-Principal, J. L. Quiles, C. L. Ramirez-Tortosa, P. Sanchez-Rovira and M. C. Ramirez-Tortosa, *Nutr. Rev.*, 2010, **68**, 191–206.
38 L. Zaharani, P. Mihankhah, M. R. Johan and N. G. Khaligh, *Catal. Lett.*, 2024, **154**, 2314–2327.
39 S. S. Smail, *Cureus*, 2024, **16**, e68280.
40 A. Qadeer, M. Anis, G. R. Warner, C. Potts, G. Giovanoulis, S. Nasr, D. Archundia, Q. Zhang, Z. Ajmal and A. C. Tweedale, *Green Chem.*, 2024, **26**, 5635–5683.
41 E. Hernández-García, M. Vargas, A. Chiralt and C. González-Martínez, *Foods*, 2022, **11**, 243.
42 P. A. Freitas, C. González-Martínez and A. Chiralt, *Polymers*, 2024, **16**, 1474.
43 T. A. Oliveira, R. R. Oliveira, R. Barbosa, J. B. Azevedo and T. S. Alves, *Carbohydr. Polym.*, 2017, **168**, 52–60.
44 S. Muniyasamy, O. Ofosu, M. J. John and R. D. Anandjiwala, *J. Renewable Mater.*, 2016, **4**, 133–145.
45 N. Nomadolo, O. E. Dada, A. Swanepoel, T. Mokhena and S. Muniyasamy, *Polymers*, 2022, **14**, 1894.
46 T. Kamal El-Sawah, R. Mohamed El-Shahawy, A. Ibrahim Nageeb and K. Mohamed Atalla, *Fayoum j. Agr. res. dev.*, 2024, **38**, 45–55.
47 S. Grabska-Zielińska, *Processes*, 2024, **12**, 2329.
48 X. Zhao, T. Chen, J. Liu, X. Wang and Y. Weng, *Food Chem.*, 2025, **463**, 141116.
49 O. B. G. Assis, D. de Britto and L. A. Forato, Embrapa Instrumentação Agropecuária, *Boletim de Pesquisa e Desenvolvimento*, 2009, p. 29.
50 R. C. dos Reis, I. A. Devilla, P. C. Correa, G. H. H. de Oliveira and V. C. de Castro, *Afr. J. Agric. Res.*, 2015, **10**, 1164–1170.
51 H. Guo, Y. Xu, H. Chen, X. Si, M. Zhou and E. Zhu, *Food Packag. Shelf Life*, 2024, **42**, 101258.
52 S. Hajji, I. Younes, S. Affes, S. Boufi and M. Nasri, *Food Hydrocolloids*, 2018, **83**, 375–392.
53 C. Han, Y. Zhao, S. W. Leonard and M. G. Traber, *Postharvest Biol. Technol.*, 2004, **33**, 67–78.
54 V. Namasivayam Sukumaar, S. Arjunan, L. N. Pandiaraj and A. Narayanan, *J. Thermoplast. Compos. Mater.*, 2024, 08927057241255883.
55 T. de Moraes Crizel, A. de Oliveira Rios, V. D. Alves, N. Bandarra, M. Moldão-Martins and S. H. Flôres, *Food Hydrocolloids*, 2018, **74**, 139–150.